

Heteropolynuclear Complexes of 3,5-Dimethylpyrazolate [Pt₂M₄(Me₂pz)₈] (M = Ag, Cu). Highly Luminescent Character of the Triplet Excited State Based on Mixed-Metal Cores

Keisuke Umakoshi,^{*,†} Takashi Kojima,[†] Keizo Saito,[†] Seiji Akatsu,[†] Masayoshi Onishi,[†] Shoji Ishizaka,[‡] Noboru Kitamura,[‡] Yoshihide Nakao,[§] Shigeyoshi Sakaki,[§] and Yoshiki Ozawa[⊥]

Department of Applied Chemistry, Faculty of Engineering, Nagasaki University, Bunkyo-machi, Nagasaki 852-8521, Japan, Division of Chemistry, Graduate School of Science, Hokkaido University, Kita-ku, Sapporo 060-0810, Japan, Department of Molecular Engineering, Graduate School of Engineering, Kyoto University, Nishikyo-ku, Kyoto 615-8510, Japan, and Graduate School of Material Science, University of Hyogo, Kamigori-cho, Ako-gun, Hyogo 678-1297, Japan

Received November 24, 2007

The platinum dimer and heteropolynuclear platinum complexes of 3,5-dimethylpyrazolate, [Pt₂M₄(μ-Me₂pz)₈] [M = H (**1**), Ag (**2**), Cu (**3**)], were synthesized and structurally characterized. They exhibit yellow, sky-blue, and orange luminescence, respectively, in the solid state. The absorption bands of **2** and **3** are mainly assigned to the combination of the metal–metal-to-ligand charge-transfer and [Pt₂ → Pt₂M₄] transitions by the time-dependent density functional theory (DFT) method. DFT calculations also indicate that the emissive states of **2** and **3** are ³[Pt₂ → Pt₂Ag₄] and ³[Cu(**4**) → Pt₂Cu₄], respectively.

Because heavy-metal ions in a molecule serve to increase the intersystem crossing rate through spin–orbit coupling and reduce the forbidden character of emission from the triplet state, iridium and platinum have attracted much attention for developing new complexes showing bright luminescence at an ambient temperature. Actually many different classes of homoleptic and heteroleptic iridium complexes have been synthesized.¹ On the other hand, the development of strongly emissive platinum complexes and the study on the control of emission energies have been limited except for recent pioneering works;² for instance, emission energies were successfully controlled by changing

the constituent coinage metal ions in the heteropolynuclear platinum complexes, [Pt₂M₄(C≡CR)₈] and [Pt₂M₄(μ-C≡CPh)₄(μ-Me₂pz)₄] [M = Cu, Ag, Au; R = *tert*-butyl, phenyl, (3-OMe)C₆H₄].³ Recently, we also reported the synthesis of a heteropolynuclear complex, [Pt₂Ag₄(μ-pz)₈],⁴ by using [Pt(pz)₂(pzH)₂] (pzH = pyrazole).⁵ However, the number of brightly luminescent platinum-based complexes is still limited, and the nature of the emissive state has not been fully understood. It is thus interesting and challenging to develop new materials of platinum or platinum-based mixed-metal complexes and to characterize their emissive state. In this Communication, we report the synthesis of a platinum complex of 3,5-dimethylpyrazolate (Me₂pz), [[Pt(Me₂pz)₂(Me₂pzH)₂]₂] (**1**), and the Me₂pz-bridged Pt₂Ag₄ and Pt₂Cu₄ analogues, [Pt₂M₄(μ-Me₂pz)₈] [M = Ag (**2**), Cu (**3**)], which exhibit bright visible-light luminescence.

The mixed-metal complexes **2** and **3** can be obtained by replacing the protons, involved in hydrogen bonds in **1**, with either a Ag^I or Cu^I ion (Scheme 1). The outstanding features of the precursor complex **1** and mixed-metal complexes **2** and **3** are that all of the complexes are brightly luminescent and that their emission energies can be controlled by the constituent coinage metal ions as follows: The complexes **1–3** exhibit bright luminescence of yellow (λ_{max} = 556 nm), sky blue (λ_{max} = 497 nm), and orange (λ_{max} = 625 nm),

* To whom correspondence should be addressed. E-mail: kumks@nagasaki-u.ac.jp.

[†] Nagasaki University.

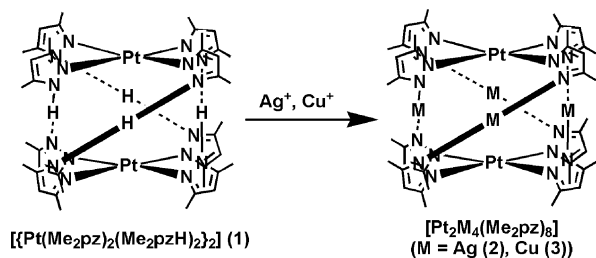
[‡] Hokkaido University.

[§] Kyoto University.

[⊥] University of Hyogo.

- (1) Lowry, M. S.; Bernhard, S. *Chem.—Eur. J.* **2006**, *12*, 7970–7977.
- (2) (a) Wadas, T. J.; Wang, Q.-M.; Kim, Y.-j.; Flaschenreim, C.; Blanton, T. N.; Eisenberg, R. *J. Am. Chem. Soc.* **2004**, *126*, 16841–16849. (b) Ma, B.; Li, J.; Djurovich, P. I.; Yousufuddin, M.; Bau, R.; Thompson, M. E. *J. Am. Chem. Soc.* **2005**, *127*, 28–29. (c) Castellano, F. N.; Pomestchenko, I. E.; Shikhova, E.; Hua, F.; Muro, M. L.; Rajapakse, N. *Coord. Chem. Rev.* **2006**, *250*, 1819–1828.

- (3) (a) Yam, V. W.-W.; Yu, K.-L.; Cheung, K.-K. *J. Chem. Soc., Dalton Trans.* **1999**, 2913–2915. (b) Charmant, J. P. H.; Forniés, J.; Gómez, J.; Lalinde, E.; Merino, R. I.; Moreno, M. T.; Orpen, A. G. *Organometallics* **1999**, *18*, 3353–3358. (c) Ara, I.; Forniés, J.; Gómez, J.; Lalinde, E.; Moreno, M. T. *Organometallics* **2000**, *19*, 3137–3144. (d) Yam, V. W.-W.; Hui, C.-K.; Yu, S.-Y.; Zhu, N. *Inorg. Chem.* **2004**, *43*, 812–821. (e) Gil, B.; Forniés, J.; Gómez, J.; Lalinde, E.; Martín, A.; Moreno, M. T. *Inorg. Chem.* **2006**, *45*, 7788–7798. (f) Forniés, J.; Fuertes, S.; Martín, A.; Sicilia, V.; Lalinde, E.; Moreno, M. T. *Chem.—Eur. J.* **2006**, *12*, 8253–8266.
- (4) Umakoshi, K.; Yamauchi, Y.; Nakamiya, K.; Kojima, T.; Yamasaki, M.; Kawano, H.; Onishi, M. *Inorg. Chem.* **2003**, *42*, 3907–3916.
- (5) Burger, W.; Strähle, J. Z. *Anorg. Allg. Chem.* **1986**, *539*, 27–32.

Scheme 1. Synthesis of $[\text{Pt}_2\text{M}_4(\text{Me}_2\text{pz})_8]$ [$\text{M} = \text{Ag}$ (**2**), Cu (**3**)]

respectively, in the solid state upon exposure to UV radiation (Figure 1).⁶ However, the emission bands of these complexes in CH_2Cl_2 solutions are significantly red-shifted from those in the solid state, with the differences in λ_{max} being 1320 cm^{-1} for **1**, 1180 cm^{-1} for **2**, and 3800 cm^{-1} for **3**. These observations may be attributed to the large structural changes in the excited state. In the excited states of **2** and **3**,⁷ the shortening of $\text{M}\cdots\text{M}$ distances and concomitant elongation of the $\text{Pt}\cdots\text{Pt}$ distance are expected because the lowest unoccupied molecular orbitals (LUMOs) involve stronger bonding interaction among coinage metal atoms, as will be discussed below. The large structural difference between the ground and photoexcited states is unfavorable for bright luminescence.⁸ However, **2** and **3** indeed exhibit bright emission with very high quantum yields in the solid state ($\Phi = 0.06$ for **1**; $\Phi = 0.85$ for **2**; $\Phi = 0.28$ for **3**), though the emission intensities are reduced in CH_2Cl_2 ($\Phi = 0.001$ and $\tau = 210\text{ ns}$ for **1**; $\Phi = 0.51$ and $\tau = 6.0\text{ }\mu\text{s}$ for **2**; $\Phi = 0.042$ and $\tau = 11.9\text{ }\mu\text{s}$ for **3**). Although a similar dependence of the emission energies on the constituent coinage metal ions was also observed for $[\text{Pt}_2\text{M}_4(\mu\text{-C}\equiv\text{CPh})_4(\mu\text{-Me}_2\text{pz})_4]$ ($\text{M} = \text{Cu}, \text{Ag}, \text{Au}$), **3** exhibits a considerably large Stokes shift in a CH_2Cl_2 solution. It is noted that the quantum yields of **2** and **3** in CH_2Cl_2 are 15–20 times higher than those of $[\text{Pt}_2\text{M}_4(\mu\text{-C}\equiv\text{CPh})_4(\mu\text{-Me}_2\text{pz})_4]$ with the corresponding coinage metal ions.^{3f}

The molecular structures of **1–3** were determined by single-crystal X-ray structure analyses.⁹ Complex **1** is given as a dimer

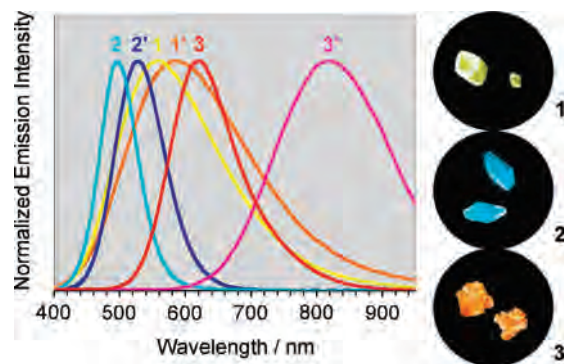


Figure 1. Normalized emission spectra of **1** [$\lambda_{\text{max}} = 556\text{ nm}$ ($18\,000\text{ cm}^{-1}$)], **2** [$\lambda_{\text{max}} = 497\text{ nm}$ ($20\,100\text{ cm}^{-1}$)], and **3** [$\lambda_{\text{max}} = 625\text{ nm}$ ($16\,000\text{ cm}^{-1}$)] in the solid state and in CH_2Cl_2 [**1'** [$\lambda_{\text{max}} = 600\text{ nm}$ ($16\,700\text{ cm}^{-1}$)], **2'** [$\lambda_{\text{max}} = 528\text{ nm}$ ($18\,900\text{ cm}^{-1}$)], and **3'** [$\lambda_{\text{max}} = 820\text{ nm}$ ($12\,200\text{ cm}^{-1}$)] at 295 K obtained by using the fourth-harmonic generation of a Nd:YAG laser at 266 nm . The photographs show luminescence of crystals of **1–3** upon exposure to UV radiation at an ambient temperature.

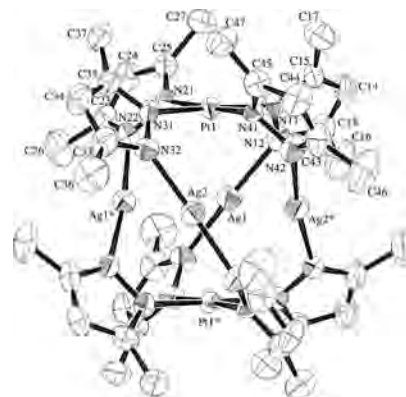


Figure 2. Molecular structure of **2** with the atomic labeling scheme (50% probability ellipsoids). Selected bond distances (\AA) and angles (deg): $\text{Pt}\cdots\text{Pt}^*$, $5.1578(8)$; $\text{Pt}\cdots\text{Ag}1$, $3.5147(8)$; $\text{Pt}\cdots\text{Ag}1^*$, $3.4514(7)$; $\text{Pt}\cdots\text{Ag}2$, $3.4980(8)$; $\text{Pt}\cdots\text{Ag}2^*$, $3.5068(8)$; $\text{Ag}1\cdots\text{Ag}1^*$, $3.285(1)$; $\text{Ag}1\cdots\text{Ag}2$, $4.711(1)$; $\text{Ag}1\cdots\text{Ag}2^*$, $3.384(1)$; $\text{Ag}2\cdots\text{Ag}2^*$, $3.272(1)$; $\text{Pt}\cdots\text{N}$, $1.972(8)\text{--}2.025(7)$; $\text{Ag}\cdots\text{N}$, $2.080(8)\text{--}2.090(8)$; $\text{N}12\cdots\text{Ag}1\text{--}\text{N}22^*$, $172.3(3)$; $\text{N}32\cdots\text{Ag}2\text{--}\text{N}42^*$, $171.0(3)$.

of mononuclear complex units, $\{\text{Pt}(\text{Me}_2\text{pz})_2(\text{Me}_2\text{pzH})_2\}$, in which two Me_2pz anions and two neutral Me_2pzH ligands coordinate to the Pt^{II} ion (Figure S1 in the Supporting Information). This dimeric structure is stabilized by the strong $\text{N}\cdots\text{H}\cdots\text{N}$ hydrogen-bonding interactions. The $\text{Pt}\cdots\text{Pt}$ distance in **1** is $3.7205(3)\text{ \AA}$, which is too long to consider an effective metal–metal interaction. The structure of $[\text{Pt}_2\text{Ag}_4(\mu\text{-Me}_2\text{pz})_8]$ (**2**) in Figure 2 is similar to those of $[\text{Pt}_2\text{Ag}_4(\mu\text{-pz})_8]$ ⁴ and $[\text{Pd}_2\text{Ag}_4(\mu\text{-Me}_2\text{pz})_8]$.¹⁰ The $\text{Pt}\cdots\text{Pt}$ distance in **2** is $5.1578(8)\text{ \AA}$. The $\text{Pt}\cdots\text{Ag}$ distances in **2** are close to each other, ranging from $3.4514(7)$ to $3.5147(8)\text{ \AA}$. The proximate $\text{Ag}\cdots\text{Ag}$ distances range from $3.272(1)$ to $3.384(1)\text{ \AA}$. The structure of **3** is very similar to that of **2** (Figure S2 in the Supporting Information). However, mainly because of the smaller ionic radius of Cu^{I} , the $\text{Pt}\cdots\text{Pt}$ distance in **3** is $4.709(1)\text{ \AA}$. The $\text{Pt}\cdots\text{Cu}$ and $\text{Cu}\cdots\text{Cu}$ distances are $3.3726(7)$ and $3.415(2)\text{ \AA}$, respectively. Although the $\text{Pt}\cdots\text{Pt}$ and $\text{Pt}\cdots\text{M}$ ($\text{M} = \text{Ag}, \text{Cu}$) distances in **2** and **3** are considerably different from those in $[\text{Pt}_2\text{M}_4(\text{C}\equiv\text{CR})_8]$ with the corresponding coinage metal ions, the $\text{Ag}\cdots\text{Ag}$ and $\text{Cu}\cdots\text{Cu}$ distances in the two systems are comparable.³

(10) Ardizzoia, G. A.; La Monica, G.; Cenini, S.; Moret, M.; Masciocchi, N. *J. Chem. Soc., Dalton Trans.* **1996**, 1351–1357.

(6) The successful analyses of emission decay curves for **1–3** by a single exponential function indicate that each emission band corresponds to a single transition. Half-width (cm^{-1}): **1**, 5690 ; **1'**, 6130 ; **2**, 2740 ; **2'**, 3170 ; **3**, 3060 ; **3'**, 3060 .

(7) The optimized geometrical parameters for the excited states of **2** and **3** are summarized in Tables S11 and S12 in the Supporting Information with those for their ground states. Selected molecular orbitals of the triplet states for **2** and **3** by the B3LYP method are also depicted in Figures S18 and S19 in the Supporting Information.

(8) Sasaki, Y. Private communication, 2006.

(9) X-ray diffraction data were collected on a Quantum CCD area detector coupled with a Rigaku AFC7 diffractometer (**1** and **2**) and Rigaku RAXIS-RAPID imaging plate (**3**) with graphite-monochromated $\text{Mo K}\alpha$ radiation ($\lambda = 0.7107\text{ \AA}$). Crystal data for **1**: $\text{C}_{40}\text{H}_{60}\text{N}_{16}\text{Pt}_2$, monoclinic, space group $C2/c$ (No. 15), $a = 17.285(1)\text{ \AA}$, $b = 15.753(2)\text{ \AA}$, $c = 17.4782(3)\text{ \AA}$, $\beta = 100.3796(4)^\circ$, $V = 4681.2(5)\text{ \AA}^3$, $Z = 4$, $T = 296\text{ K}$, $D_{\text{calcd}} = 1.639\text{ g cm}^{-3}$, $\mu(\text{Mo K}\alpha) = 59.93\text{ cm}^{-1}$, $R(F_o^2) = 0.057$, $R_w(F_o^2) = 0.069$. Crystal data for **2**: $\text{C}_{40}\text{H}_{56}\text{Ag}_4\text{N}_{16}\text{Pt}_2$, monoclinic, space group $C2/c$ (No. 15), $a = 20.831(2)\text{ \AA}$, $b = 12.924(2)\text{ \AA}$, $c = 19.4719(3)\text{ \AA}$, $\beta = 105.1428(4)^\circ$, $V = 5060.3(8)\text{ \AA}^3$, $Z = 4$, $T = 296\text{ K}$, $D_{\text{calcd}} = 2.077\text{ g cm}^{-3}$, $\mu(\text{Mo K}\alpha) = 70.44\text{ cm}^{-1}$, $R(F_o^2) = 0.087$, $R_w(F_o^2) = 0.159$. Crystal data for **3**: $\text{C}_{40}\text{H}_{56}\text{Cu}_4\text{N}_{16}\text{Pt}_2$, tetragonal, space group $I422$ (No. 97), $a = 13.4338(7)\text{ \AA}$, $c = 13.8003(8)\text{ \AA}$, $V = 2490.5(2)\text{ \AA}^3$, $Z = 2$, $T = 296\text{ K}$, $D_{\text{calcd}} = 1.874\text{ g cm}^{-3}$, $\mu(\text{Mo K}\alpha) = 73.18\text{ cm}^{-1}$, $R(F_o^2) = 0.0985$, $R_w(F_o^2) = 0.0968$.

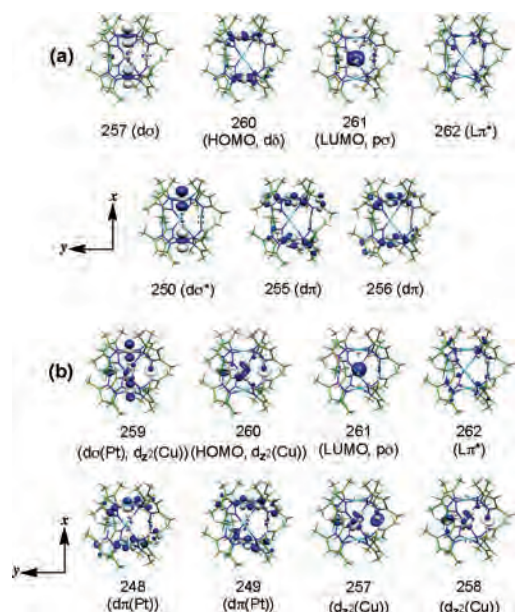


Figure 3. Isosurface plots ($\psi = \pm 0.05$ atomic units) of selected molecular orbitals important to the band assignment for **2** (a) and **3** (b).

To shed clear light on the absorption spectra of **2** and **3**, the absorption bands of these complexes were theoretically investigated with the time-dependent density functional theory (DFT) method. Those of pz analogues were also investigated because $[\text{Pt}_2\text{Ag}_4(\mu\text{-pz})_8]$ does not exhibit emission in the solid state and in a fluid solution. Calculated transition energies agree well with the experimental results in Table S7 in the Supporting Information. This table summarizes the excitations (transitions) with strong oscillator strengths, which have a higher contribution to the absorption spectra of **2** and **3**. The molecular orbitals, which contribute to the excitations in this table, are depicted in Figure 3. The absorption bands of **2** are assigned to the combination of the metal–metal-to-ligand charge-transfer (MMLCT) and $[\text{Pt}_2 \rightarrow \text{Pt}_2\text{Ag}_4]$ transitions,¹¹ where the former involves transitions from $d\pi(\text{Pt})$ and $d\sigma(\text{Pt})$ to π^* of Me_2pz ligands and the latter involves transitions from $d\sigma^*(\text{Pt})$, $d\pi(\text{Pt})$, and $d\pi^*(\text{Pt})$ to the LUMO; see Figure 3 for these orbitals. The absorption bands of **3** are similarly assigned to those of **2**, but they also involve transitions from Cu(d) to the LUMO ($[\text{Cu}(\text{d}) \rightarrow \text{Pt}_2\text{Cu}_4]$). The LUMO mainly consists of in-phase combination of 6p of two Pt ions and 5p of four Ag ions (or 4p of four Cu ions). The in-phase combination among coinage metal ions and Pt^{II} ions is reported here for the first time in the heteropolynuclear Pt^{II} complexes, though that of $(n+1)s$ orbitals of Cu, Ag, and Au ($n = 3-5$) is observed in the LUMO of $[\text{M}_3\{3,5\text{-(CF}_3)_2\text{pz}\}_3]$.¹²

The triplet excited state was optimized with the DFT method because the emission takes place from the triplet state in these complexes. The calculated energies of emission agree well with the experimental values for **2** and **3**.¹³

The emission of **2** is assigned to the transition from the in-phase combination of 6p(Pt) and 5p(Ag) to the $d\delta(\text{Pt})$ nonbonding orbital ($^3[\text{Pt}_2 \rightarrow \text{Pt}_2\text{Ag}_4]$). The singly occupied molecular orbitals (SOMOs) obtained for the triplet excited state of **2** are similar to the LUMO and highest occupied molecular orbital of the ground state. In **3**, one SOMO also consists of the in-phase combination of 6p(Pt) and 4p(Cu) like that of **2**, but the other consists of a $d\pi(\text{Cu})$ orbital localized on one of the four Cu ions. The emission of **3** is assigned as the emission from the $^3[\text{Cu}(\text{d}) \rightarrow \text{Pt}_2\text{Cu}_4]$ excited state. The difference in the SOMOs between **2** and **3** is interpreted in terms of the difference in the orbital energies of Ag, Cu, and Pt as follows: The 3d orbital of Cu^{I} is located at energy higher than the 5d orbital of Pt^{II} , and the 4d orbital of Ag^{I} is located at energy lower than the 5d orbital of Pt^{II} (Figure S21 in the Supporting Information). Thus, one SOMO of **2** consists of the 5d orbital of Pt^{II} , while that of **3** becomes the 3d orbital of Cu^{I} , though the rest of the SOMOs in **2** and **3** are similar to their LUMOs. As is seen in the assignments of absorption bands, the emissive states of **2** are also essentially the same as those of pz analogues, even though the introduction of methyl groups on the pyrazolate ligand is found to result in dramatic enhancement in the luminescence quantum yield. The studies for elucidating the effect of the substituent groups on the luminescent properties are in progress.

In conclusion, brightly luminescent platinum dimer and heteropolynuclear platinum complexes, $[\text{Pt}_2\text{M}_4(\mu\text{-Me}_2\text{pz})_8]$ [$\text{M} = \text{H}$ (**1**), Ag (**2**), Cu (**3**)], are prepared and structurally characterized. The yellow, sky-blue, and orange luminescences of **1–3**, respectively, indicate that the emission energy can be controlled by the change of incorporated cations. DFT calculations show that **2** and **3** have quite unique LUMOs. The observed lifetimes of the emission in the microsecond regime are consistent with the assignment that the emissive states of **2** and **3** are $^3[\text{Pt}_2 \rightarrow \text{Pt}_2\text{Ag}_4]$ and $^3[\text{Cu}(\text{d}) \rightarrow \text{Pt}_2\text{Cu}_4]$, respectively.

Acknowledgment. The authors are grateful to Dr. Kiyoshi Tsuge at Hokkaido University for measurements of quantum yields in the solid state. This work was partially supported by a Grant-in-Aid for Scientific Research.

Note Added after ASAP Publication. This paper was released ASAP on May 6, 2008 with minor errors in the text. The correct version was posted on May 13, 2008.

Supporting Information Available: Experimental details and characterization data including crystallographic data in CIF format. This material is available free of charge via the Internet at <http://pubs.acs.org>.

IC702310T

(11) Here we define the term “MMLCT” as the charge-transfer transition from $\sigma(\text{Pt-Pt})$ to ligand π^* orbitals. A $[\text{Pt}_2 \rightarrow \text{Pt}_2\text{Ag}_4]$ transition means that the excitation occurs from the $\sigma^*(\text{Pt-Pt})$ orbital to the bonding orbital of the Pt_2Ag_4 moiety: see the 261 molecular orbital for Pt_2Ag_4 and the 250 molecular orbital for $\sigma^*(\text{Pt-Pt})$. Note that the 261 molecular orbital consist of the bonding combination of 6p of Pt atoms and 5p of Ag atoms.

(12) (a) Dias, H. V. R.; Diyabalanage, H. V. K.; Eldabaja, M. G.; Elbjeirami, O.; Rawashdeh-Omary, M.; Omary, M. A. *J. Am. Chem. Soc.* **2005**, *127*, 7489–7501. (b) Omary, M. A.; Rawashdeh-Omary, M.; Gonsler, M. W. A.; Elbjeirami, O.; Grimes, T.; Cundari, T. R. *Inorg. Chem.* **2005**, *44*, 8200–8210.

(13) Calculated emission energies: **2**, 2.54 eV (488 nm); **3**, 1.53 eV (810 nm), where structural relaxation was considered in the calculation.